Short Communication

Effect of Er on the Characteristics of an Oxide Coating Prepared by Micro-Arc Oxidation on a 7075 Aluminum Alloy

XianJu Zhang, Xia Luo, WuXing Ou, JunJie Huang, YangYang Li*

School of Materials Science and Engineering, Southwest Petroleum University, Chengdu 610500, China
*E-mail: zhangxj701@163.com

7075 Aluminum alloys with 0% (wt.%), 0.15% and 0.30% Er were subjected to micro-arc oxidation under the same parameters. The surface morphology and the phases of the oxide coating were analyzed using SEM and XRD. The microhardness, thickness and corrosion resistance of the oxide coating were also studied. The results show that the micro-arc oxidation coating on a 7075 aluminum alloy with different Er contents is composed of the gamma-Al_2O_3 phase. With increasing Er content, the peak of the gamma-Al_2O_3 phase becomes stronger. Er enters the oxide coating in the form of $Al_{17}Er_2$, which is an unbalanced phase under micro-arc oxidation. With increasing Er content, the surface deposits become finer and more uniform, the microhole diameter decreases, and the flatness increases. As the Er content increases from 0% to 0.30%, the micro-hardness and thickness of the oxide coating also increase, and then the corrosion resistance increases significantly. Consequently, the self-corrosion current density decreases from 4280.0 nA/cm^2 to 2.405 nA/cm^2.

1. INTRODUCTION

Aluminum alloys are widely used in the aviation, aerospace and civil industries due to their high strength, low density and good hot workability, but its low hardness and poor corrosion resistance limit its application [1-2]. Micro-arc oxidation (MAO) is a new environmental protection technology. It can form a ceramic layer on the surface of light metals such as aluminum, magnesium, titanium and their alloys, thus improving the hardness, corrosion resistance and other properties of the alloys. It is an effective surface treatment method.

Rare earth elements can improve the sintering performance, toughness and compactness of ceramics [3-5]. Therefore, many researchers have studied the effect of rare earth elements on the properties of micro-arc oxidation ceramic coatings. Rare earth elements, such as Ce, La, and Y, play

three roles in a micro-arc oxidation coating, serving as alloying elements, electrolyte additives, and pretreatment solutions for soaking alloys. Many researchers have focused on rare earth elements as pretreatment solutions or additives [6-10]. The results prove that a certain rare earth content can improve the hardness, wear resistance and corrosion resistance of oxidation coatings. However, there are only a few studies on rare earth elements as alloying elements, especially those containing Er. Wang [11] studied the structure and properties of a micro-arc oxidation coating of Mg-11Gd-1Y-0.5Zn alloy. It was found that the addition of rare earth elements only affected the phase composition of the oxide coating, therefore improving the corrosion resistance. However, no crystal phase containing the rare earth element was found in the oxide coating. Cai [12] studied the corrosion resistance of the micro-arc oxidation coating of AZ91 alloy with Ce contents of 0%, 0.92% and 1.8%. It was found that Ce could promote the formation process and improve the corrosion resistance of the oxidation coating, but no rare earth phase was found in the coating. Ren [13] found that the mass fraction of Y in magnesium alloy had a great influence on its wear resistance, and no phase containing Y was found in the oxide coating when the content of Y reached 2%. All these studies show that the rare earth elements in the matrix have a positive effect on the properties of micro-arc oxidation coatings. However, it remains unclear whether rare earth elements enter the oxidation coating and how they affect the formation process of the coating. Therefore, MAO-coated ceramic coatings that have been prepared on AA7075 aluminum alloy with different Er contents are studied, and the effect of Er on the composition and properties of the oxide coatings is also studied.

2. MATERIALS AND EXPERIMENTAL METHODS

The raw materials used are 7075 aluminum alloy and Al-15%Er intermediate alloy. It was melted in a vacuum furnace, and after being poured and homogenized, hot rolling was used. Then, cold rolling and a T6 treatment were performed to obtain the AA7075-Er aluminum alloy. The chemical composition is shown in Table 1. The specimen was cut into a rectangular sheet with dimensions of 20 mm×10 mm×3 mm, polished, unoiled, rinsed with deionized water, and cleaned by ultrasonication.

Table 1. Compositions of the alloys (wt.%)

composition	Zn	Mg	Cu	Cr	Er	Fe	Si	Mn	Al
sample 1	5.61	2.42	1.43	0.22	0	0.08	0.06	0.05	balance
sample 2	5.66	2.40	1.45	0.24	0.15	0.07	0.06	0.05	balance
sample 3	5.57	2.50	1.41	0.27	0.30	0.09	0.05	0.06	balance

The aluminum alloy sample served as the anode, and a stainless steel container was the cathode. Micro-arc oxidation was carried out using a constant current-pulse device with a power of 5 kW. The electrolyte was composed of 10 g/L Na_2SiO_3, 3 g/L NaOH, and 1 g/L $NaAlO_2$. The current density used was 6 A/dm^2, with a duty ratio of 20%, frequency of 100 Hz, and oxidation time of 30 min. The

electrolyte temperature was controlled below 30°C. The samples were washed with deionized water and then dried. The morphology of the micro-arc oxide coating was observed by scanning electron microscopy (SEM, HITACHI S-450). The phase composition was analyzed by X-ray diffraction (XRD, XPertPRO). Diffraction data were acquired over 2θ scattering angles of 10° to 70° and a scanning speed of 0.1°/s. The thickness was measured by a pachymeter (TT230), and the microhardness was measured by a hardenometer (HVS-1000) at 1 N for 15 s. The polarization curve of the oxide coating was tested by an electrochemical workstation (IM6) in a 3.5% NaCl solution at room temperature with a range of -1.1 V to -0.2 V and a scanning rate of 1.5 mV·s^{-1}.

3. RESULTS AND DISCUSSION

3.1 Phase composition

Fig. 1 shows the XRD pattern of the micro-arc oxidation coatings of 7075 aluminum alloy with different Er contents. The microarc oxidation coating is mainly composed of gamma-Al_2O_3, where Al comes from the matrix but without Er. It may be that the level of Er is too low and the sensitivity of the instrument is not high enough to detect it. The count of the gamma-Al_2O_3 phase peak for each sample is observed. The peak of the gamma-Al_2O_3 phase is enhanced with increasing Er content. To determine the effect of Er on the Al_2O_3 phase and whether the reaction of Er was involved, MAO was carried out on the Al-15%Er intermediate alloy (as shown in Fig. 2). The coating of the sample is almost entirely composed of the $Al_{17}Er_2$ phase (PDF: 00-047-1121).

The appearance of Al also comes from the matrix, but the Al_2O_3 phase is not observed. This indicates that Al_2O_3 is not the preferred phase, and when the Er content remains stable, the Al_2O_3 phase will be completely inhibited. According to the Al-Er binary phase diagram [14] and the results from Ref. [15-17], the Er in aluminum alloy mainly exists in the formation of Al_3Er, but the $Al_{17}Er_2$ phase is not observed. Therefore, it can be speculated that the $Al_{17}Er_2$ phase is a non-equilibrium phase produced by micro-arc oxidation, and the following reaction may occur:

$$2Al_3Er+11Al \longrightarrow Al_{17}Er_2$$

Song [18] studied the micro-arc oxidation coating of an AZ91 alloy containing Nd and found that Nd existed as Al_2Nd in the alloy matrix but formed Nd_2O_3 in the ceramic coating under micro-arc oxidation. The results in this paper are different from them. Al_3Er in the matrix is not oxidized to Er_2O_3 but to $Al_{17}Er_2$.

For 7075 aluminum alloys with Er contents of 0.15% and 0.30%, the formation of the $Al_{17}Er_2$ phase occurs prior to that of the Al_2O_3 phase during micro-arc oxidation, and then the $Al_{17}Er_2$ phase becomes the crystal nucleus of the molten Al_2O_3 phase. However, it is not observed in the XRD pattern due to its low amount.
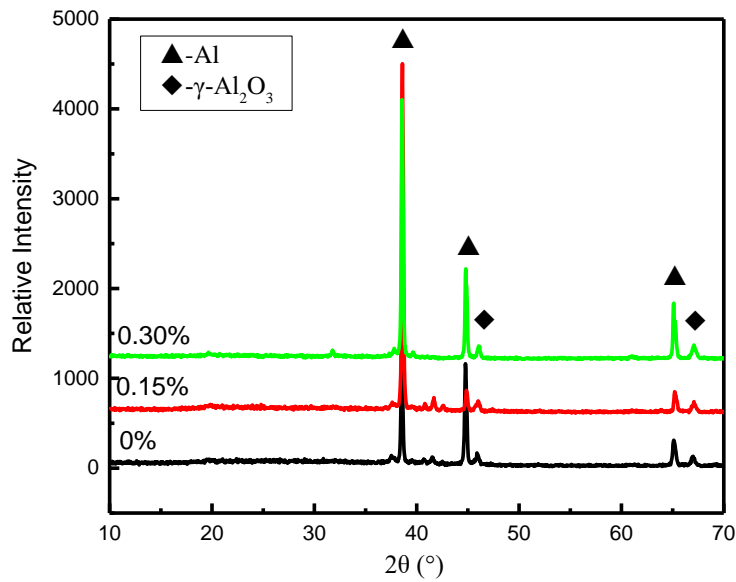
Figure 1. XRD patterns of the MAO coating on 7075 alloys with different Er contents
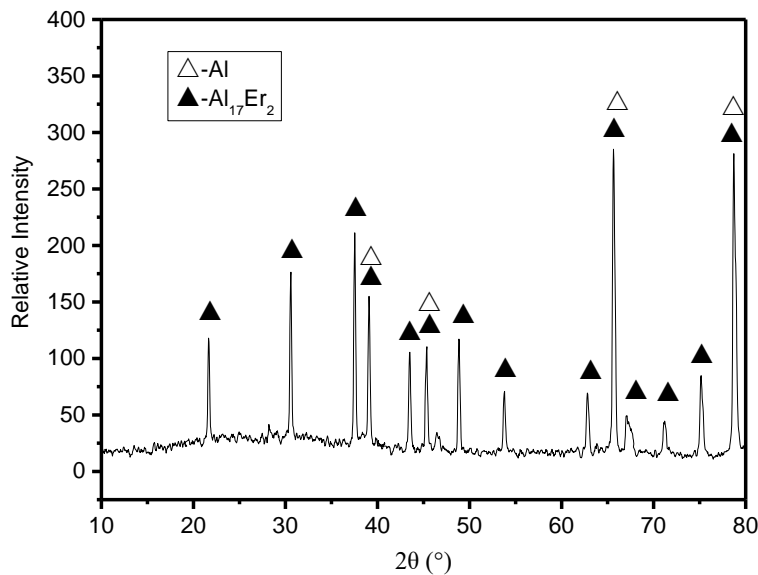

Figure 2. XRD patterns of the MAO coating with Al-15%Er

3.2 Surface morphology

The surface morphology of the samples after micro-arc oxidation is shown in Fig. 3. It can be seen from the figure that holes, which look similar to "craters", appear on the surface of the samples after micro-arc oxidation. The surface oxide film is broken down to form a discharge channel. Melting Al_2O_3 forms at high temperatures, then outflows and solidifies. After that, the oxide coating continues to thicken, and a large number of discharge channels accumulate, resulting in an increase in the surface roughness. With increasing Er content, the surface deposits become finer and more uniform, the

microhole diameter decreases, and the flatness increases. The difference in the surface morphology must be the involved Er content in the matrix. Under the action of a micro-arc, Er at the interface between the matrix and the oxide coating is in the melting state together with Al. Because rare earth elements are relatively active, it is easy to fill in the defects of the oxide coating so that the interfacial tension between the old and new phases decreases; the decrease in interfacial tension increases the nucleation rate of the crystal nucleus, thus forming an active surface film for preventing grain growth [19]. In addition, the formation of the intermetallic compound $Al_{17}Er_2$ is due to the rare earth Er under the action of the arc, which is ejected from the discharge channel and becomes the crystal nucleus of the ceramic coating. It greatly increases the number of ceramic crystal nuclei. Due to the role of rare earth elements in reducing the melting point of ceramics [3], the melted Al_2O_3 fully flows and penetrates into discharge channels. It increases the density of the ceramic coating and decreases the microhole diameter. Therefore, the flatness of the surface increases.
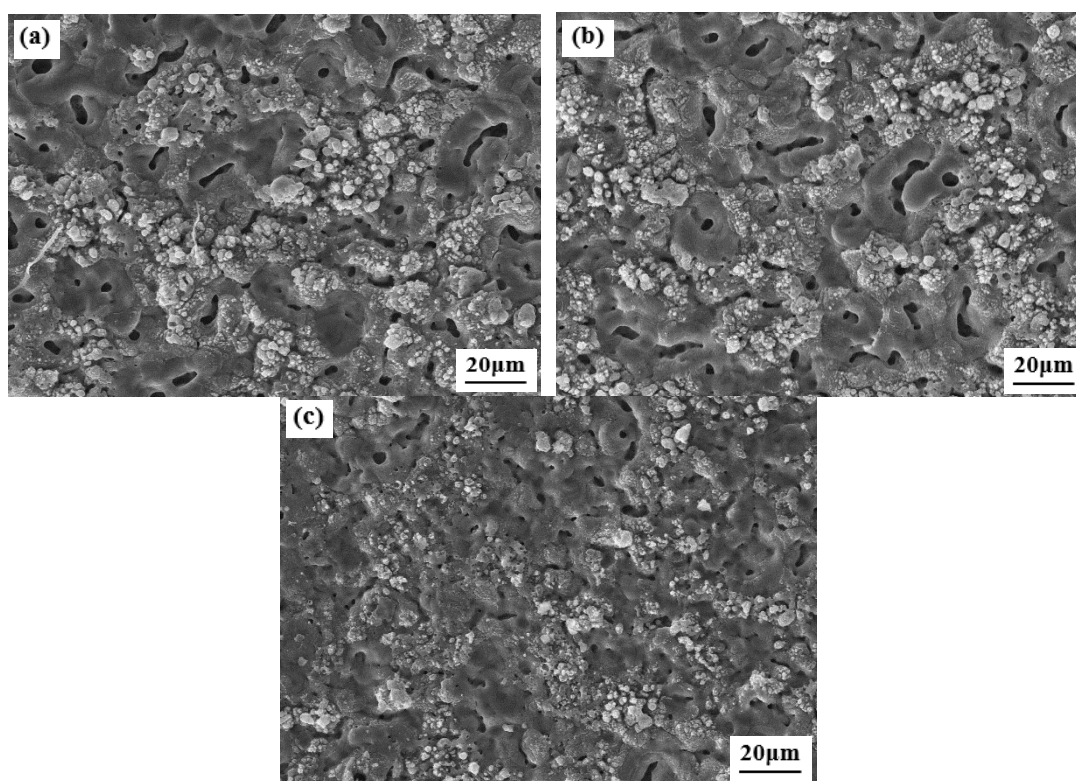

Figure 3. SEM surface morphologies of the MAO coatings on the 7075 aluminum alloys with: (a) 0% Er, (b) 0.15% Er, and (c) 0.30% Er

3.3 Hardness and thickness

The microhardness and thickness of the ceramic coating were tested, and the results are shown in Fig. 4. When the content of Er increases from 0% to 0.30%, the micro-hardness increases from 170.58 HV to 180.5 HV, and the thickness increases from 5.20 μm to 8.98 μm. Therefore, in the range of this experiment, with the increase in Er content in the matrix, both the microhardness and thickness increase. This is because the addition of rare earth Er improves the distribution law of Si, Fe and other harmful elements in the alloy [20], which are changed from the solid solution state to the precipitated state. It

reduces the resistivity and improves the conductivity [21-22]. The starting arc voltage is reduced, and the stating arc time is shortened as the arc discharge time is extended, enhancing the formation of more Al_2O_3 and increasing the thickness. Therefore, the rare earth element in the alloy is beneficial for improving the coating formation rate [23], and it accelerates the migration of the converted ions from the matrix to the surface of the coating [24]; additionally, it promotes the oxidation process, as evidenced by the increasing thickness. On the other hand, the Er element refines the microstructure of the 7075 alloy [25] and reduces the volume fraction of the second phase, which is evenly distributed in the boundary of the α-Al phase. Therefore, the composition of the alloy surface is more uniform. At the beginning of micro-arc oxidation, the potential fluctuation is small, and the arc distribution is more uniform. Then, the arc intensity and distribution on the coating surface become increasingly homogeneous. At the same time, the Er element enters the oxide layer to reduce the melting point of Al_2O_3 [3], and the melted Al_2O_3 fully flows and penetrates into the discharge channels. It increases the density of the ceramic coating and increases the hardness.
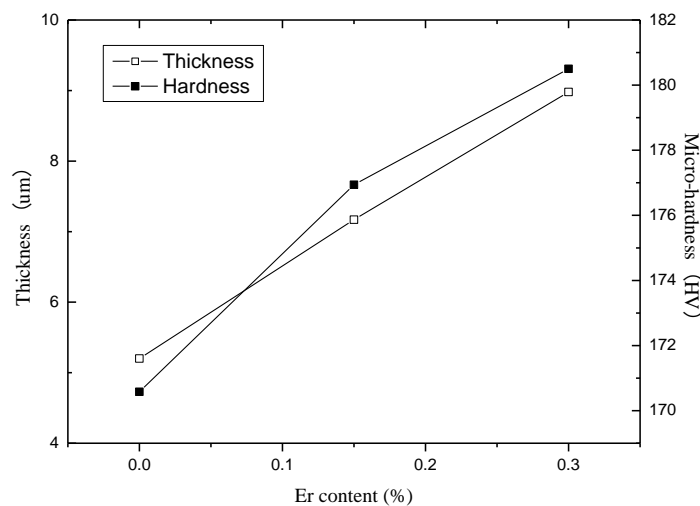

Figure 4. Hardness and thickness of the MAO coating on the 7075 alloys with different Er contents

3.4 Corrosion resistance

In this study, an electrochemical method was used to evaluate the corrosion resistance of the oxide coatings. The results of the polarization curve are shown in Fig. 5. After fitting the data, the corrosion potential and corrosion current density are obtained, as shown in Table 2. As seen from Table 2, with increasing Er content, the corrosion potential increases, and the corrosion current density decreases from 4.280×10^{-6} A/cm^2 to 2.405×10^{-9} A/cm^2. In other words, when the amount of Er is from 0% to 0.30%, the corrosion resistance of the micro-arc oxidation coating increases by approximately 2,000 times. This is because the addition of Er can increase the thickness of the oxide coating and increase the density, which greatly reduces the number of corrosion channels in the ceramic coating, so the corrosion resistance is improved.
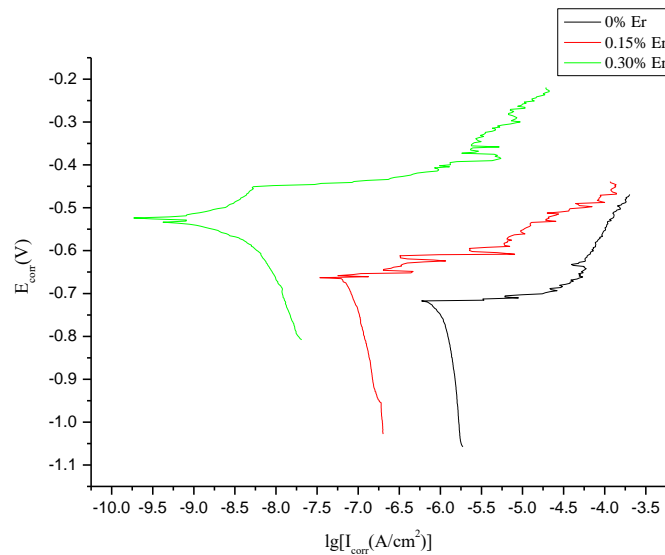
Figure 5. Polarization curves of the MAO coating with a platinum electrode for an auxiliary electrode and a calomel electrode for a reference electrode in a 3.5% NaCl solution

Table 2. Tafel fitting data of the polarization curves

Er content	corrosion current density/Icorr (A/cm^2)
0%	4.280×10^{-6}
0.15%	1.152×10^{-8}
0.30%	2.405×10^{-9}

4. CONCLUSION

(1) For a 7075 aluminum alloy with 0%, 0.15% and 0.30% Er, all the micro-arc oxidation coatings are composed of the gamma-Al_2O_3 phase. With increasing Er content, the peak of the gamma-Al_2O_3 phase becomes stronger. Er enters the oxide coating in the formation of $Al_{17}Er_2$.

(2) With increasing Er content, the surface deposits become finer and more uniform, the microhole diameter decreases, and the flatness increases.

(3) When the Er content ranges from 0% to 0.30%, the micro-hardness, thickness and corrosion resistance characteristics of the oxide coating are improved.

References

1. L.T. Duartel, B. Claudemiro, S.R. Biaggio, R. F. Romeu C and P.A.P. Pedro, *Mater. Sci.   Eng.*, C, 41(2014)343.

2. S. Zhou, L. Hui, L. Xu, Y. T. Yu and S.H. Ma, *Adv. Mater. Res*., 904(2014)86.
3. H. Cheng, P. Cheng, W.H. Xiang, *Ceram. Int.*, 45(2019)3263.
4. Y.S. Duan, J.X. Zhang, X.G. Li, M.M. Huang, Y. Shi and J.J. Xie, *J. Inorg. Mater.,* 32(2017)1275.
5. K.S. He, X.Y. Cheng, Z.H. Li, *Lubric. Eng*., 34(2009)100.
6. Y.P. Gou, S.C. Di, P.X. Lu and S.F. Sun, *Rare Metal Mat. Eng*., 44(2015)2240.
7. P. Sun, A.W. Niu, S. Xu, M.Z. Li and M.Y. Xu, *Plating and Finishing*, 37(2015)27.
8. P. Wang, T. Wu, Y. T. Xiao, J. Pu and X.Y. Guo, *Mater. Lett*. , 182(2016)27.
9. S. C. Di, Y.P. Guo, H.W. Lv, *Ceram. Int*., 41(2015)6178.
10. F. Liu, Y.J. Li, J.J. Gu, Q.S. Yan and Q. Luo, *T. Nonferr. Metal Soc*., 22(2012)1647.
11. P. Wang, J.Y. Li, Y.C. Guo and Y. Zhong, *J. Rare Earths*, 28(2010)798.
12. J.S. Cai, F.H. Cao, L.R. Chang, Z. Zhang, J.Q. Zhang and C.N. Cao, *J. Zhejiang Univ*., 45(2011) 2055.
13. X.D. Ren, Y.Y. Zhao, X.S. Li, *Electroplat. & Pollut. Control*, 35(2015)34.
14. Z.T. Wang, R.Z. Tian, Aluminum alloy and its machining manual, Cent. South Univ. Press, (2005)Chang Sha, China.
15. Y.T. Li, Z.Y. Liu, Q.K. Xia and R.C. Yu, *J. Cent. South Univ*., 37(2006)1044.
16. Y. Zhang, K.Y. Cao, S.P. Wen, H. Huang, Z.R. Nie and D.J. Zhou, *J. Alloys Compd*. , 610(2014)27.
17. S.W. Yu, W. Wang, J.J. Yang, J.X. Zhou and Z.R.Nie, *J. Chin. Soc. Rare Earths*, 24(2006)470.
18. Y.L. Song ,Y.H. Liu, S.R. Yu, X.Y. Zhu and Q. Wang，*Appl. Surf. Sci.*, 254(2008)3014.
19. C.T. Wang, W.G. Lin, H.Z. Cao and G.Q. Zheng, *Surf. Technol*., 32(2003)49.
20. H.X. Li, K.X. Song, Y.M. Zhang, B.H. Tian, F.Z. Ren and Y.F. Wang, *Heat Treat. Metals*, 43(2018)25.
21. S.C. Wang, N. Zhou, D.F. Song and D. Long, *Mater. Sci. Forum*, 898(2017)367.
22. X. Zhang, Z.H. Wang, Z.H. Zhou, J.M. Xu, *J. Wuhan Univ. Technol.,* 32(2017)611.
23. J.X. Chen, Y. Zhang, M. Ibrahim, I.P. Etim, L.L. Tan and K. Yang, *Colloids Surf.,B*,179(2019)179.
24. F.F. Jia, W. Dong, L.Y. Zhang, J.D. Li and B.J. Liu, *Mater. Rev.*, 29（2015）46.
25. Z.J. Meng, G.L. Liu, T. Zhao and Z.F. Shi, *Heat Treat. Metals,* 44(2019)31.